



LUND UNIVERSITY

Integrating Sphere Measurements of Tissue Optical Properties For Accurate Pdt Dosimetry

Nilsson, A. M. K; Berg, R; Andersson-Engels, Stefan

Published in:

Laser Interaction with Hard and Soft Tissue II, Proceedings of

DOI:

[10.1117/12.199183](https://doi.org/10.1117/12.199183)

1995

[Link to publication](#)

Citation for published version (APA):

Nilsson, A. M. K., Berg, R., & Andersson-Engels, S. (1995). Integrating Sphere Measurements of Tissue Optical Properties For Accurate Pdt Dosimetry. In HJ. Albrecht, GP. Delacretaz, TH. Meier, RW. Steiner, LO. Svaasand, MJC. vanGemert, & A. Katzir (Eds.), *Laser Interaction with Hard and Soft Tissue II, Proceedings of* (Vol. 2323, pp. 47-57). SPIE. <https://doi.org/10.1117/12.199183>

Total number of authors:

3

General rights

Unless other specific re-use rights are stated the following general rights apply:

Copyright and moral rights for the publications made accessible in the public portal are retained by the authors and/or other copyright owners and it is a condition of accessing publications that users recognise and abide by the legal requirements associated with these rights.

- Users may download and print one copy of any publication from the public portal for the purpose of private study or research.
- You may not further distribute the material or use it for any profit-making activity or commercial gain
- You may freely distribute the URL identifying the publication in the public portal

Read more about Creative commons licenses: <https://creativecommons.org/licenses/>

Take down policy

If you believe that this document breaches copyright please contact us providing details, and we will remove access to the work immediately and investigate your claim.

LUND UNIVERSITY

PO Box 117
221 00 Lund
+46 46-222 00 00

Integrating sphere measurements of tissue optical properties for accurate PDT dosimetry

Annika M. K. Nilsson, Roger Berg and
Stefan Andersson-Engels

Department of Physics, Lund Institute of Technology,
P.O. Box 118, S-221 00 Lund, Sweden
annika.nilsson@fysik.lth.se

ABSTRACT

A set-up with an integrating sphere and a narrow-beam arrangement was used in order to derive the optical properties *in vitro* of 1 mm thick tissue slabs. The measured macroscopic quantities, the reflectance and the total transmittance, were correlated to the tissue optical properties by Monte Carlo simulations. Mie calculations were performed to be able to calibrate the set-up with a solution of latex spheres and ink. Finally, the optical properties of rat liver samples were measured, before and after photodynamic therapy, showing approximately a 40 % increase of the absorption coefficient at 650 nm due to the treatment.

1. INTRODUCTION

The tissue optical properties, which characterise the interaction between light and tissue, can be described by the *g*-factor, scattering (μ_s) and absorption (μ_a) coefficient. When ignoring inelastic scattering and fluorescence, a photon interacting with the tissue has two options at every interaction site; either to be absorbed or to be further scattered. The absorption and scattering coefficient is defined as the probability of absorption and scattering, respectively, per unit infinitesimal path length. The attenuation coefficient, μ_t , is given by the sum of the absorption and scattering coefficient. Finally, the anisotropy factor, *g*, specifies the average cosine of the scattering angle, where the two opposite light distributions due to isotropic and totally forward scattering are characterised by $g=0$ and $g=1$, respectively.

These tissue characteristics are important for all kinds of medical laser applications, to understand the interaction mechanisms between light and tissue. The knowledge of light transport in tissue is particularly essential for dosimetry in conjunction with photodynamic tumour treatment, in order to follow and control the light interaction volume. It is therefore important to study what happens to the *g*-factor, scattering and absorption

coefficient during the treatment irradiation. If the treatment causes changes to the optical properties, the treatment volume, and hence the effects, will alter.

Various optical integrating sphere techniques have been developed to quantify tissue optical properties, and a number of studies have recently utilised these techniques¹⁻³.

2. MEASUREMENTS OF TISSUE OPTICAL PROPERTIES - MATERIAL AND METHODS

The three optical quantities of tissue characteristic, g , μ_s and μ_a , were determined in a three step procedure. A 1 mm thick tissue slab was put between two microscope object glasses (1 mm thickness), with 1 mm thick glass spacers in-between. The total thickness, 3 mm, of the resulting glass cuvette, was verified by a vernier calliper. The cuvette was sequentially placed at the two sample positions of the integrating sphere, measuring the reflectance and the total transmittance, respectively. Following those measurements, the collimated transmittance was measured with a narrow-beam technique. Finally, the corresponding g , μ_s and μ_a were derived by spline interpolation in a table of Monte Carlo simulated data.

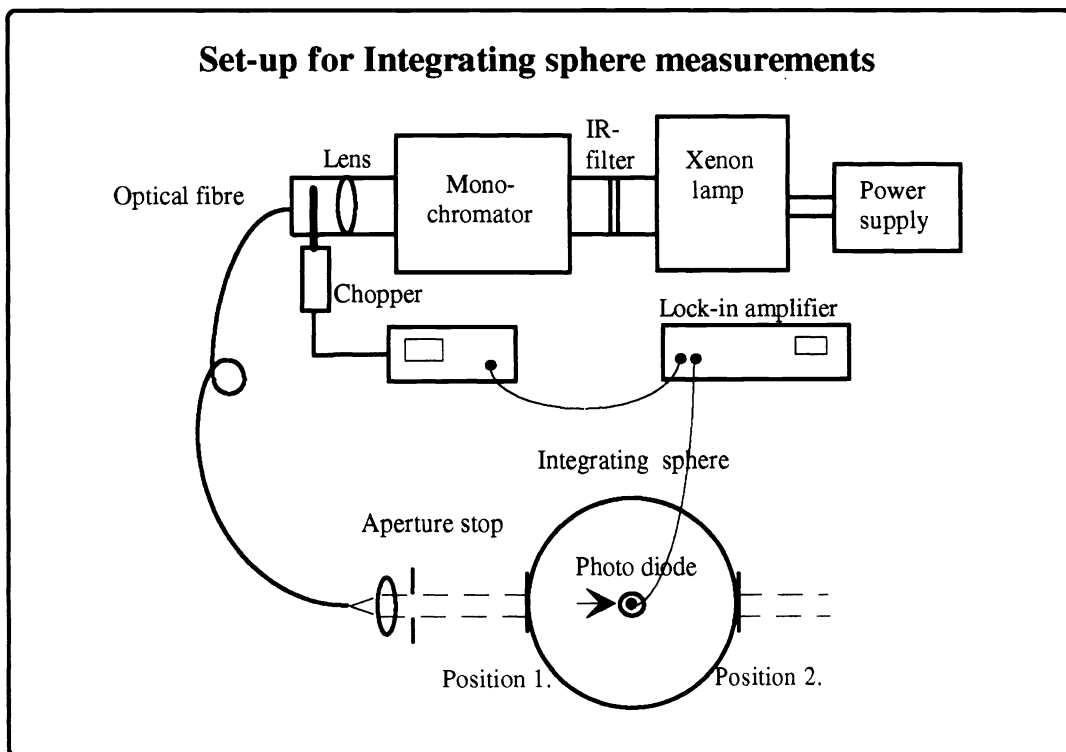


Figure 1. The total transmittance and the reflectance were measured with the tissue sample situated at the integrating sphere position 1 and 2, respectively.

2.1 Integrating sphere and narrow-beam measurements

Figure 1 shows the set-up for integrating sphere measurements. As a light source a 75 W high pressure Xenon lamp was used in combination with a monochromator to select the wavelength. The light was guided to the integrating sphere in a quartz fibre with the diameter 200 μm . A lens followed by an aperture stop formed a collimated light beam with a diameter of 5 millimetres. The beam reached the tissue slab either at the entry port of the integrating sphere for the total transmittance measurements, or at the exit port for the reflectance measurements. The integrating sphere by Oriel was 20.3 cm in diameter and its two beam ports, here called entry and exit port, was opposite to one another and had a diameter of 2.54 cm. The inner surface was covered with a highly reflecting medium, barium sulphate, which reflects the entering light so that the total light intensity spread in the sphere was measured by a photo diode. The diode was positioned in the sphere surface perpendicular to the entering light beam. The reflectance and the total transmittance were obtained by

$$R=R_{\text{BS}}\times(I_{\text{R}}/I_{\text{ref}})$$
$$T=R_{\text{BS}}\times(I_{\text{T}}/I_{\text{ref}})$$

where R_{BS} symbols the reflectance of barium sulphate and I_{R} the light intensity measured by the photo diode with the tissue sample positioned at the exit port. I_{T} is the light intensity measured with the sample at the entry port and a barium sulphate plug in the exit port. Finally, I_{ref} is the intensity measured without any sample, with the light beam entering the first port and the barium sulphate plug in the exit port.

The specularly reflected light from the tissue sample, when placed at the exit port, was blocked by a baffle mounted inside the sphere, so that this light could not interfere with the measurements of the reflectance.

A lock-in technique in combination with a light chopper was used to prevent the surrounding light from disturbing the measurements.

Figure 2 shows the radial light profile of the transmitted and reflected light at the two borders of the cuvette containing a tissue sample. This is the result of Monte Carlo simulations (see below) with $g=0.909$, $\mu_{\text{s}}=9.77 \text{ mm}^{-1}$ and $\mu_{\text{a}}=0.205 \text{ mm}^{-1}$, typical data of liver tissue measured at 650 nm. In figure 2 it can be calculated that approximately 0.1-0.2 % of the transmitted and reflected light are lost due to the limited port diameter. This ensures that the photo diode of the integrating sphere did not measure too small magnitudes of the transmittance and reflectance. J. H. Torres *et. al.* pointed out in their study⁴ that the absorption coefficient easily can be overestimated when the port-to-beam-size ratio is too low. A beam diameter of 5 mm and a port diameter of 2.54 cm, as in our case, did apparently not yield a too low port-beam ratio.

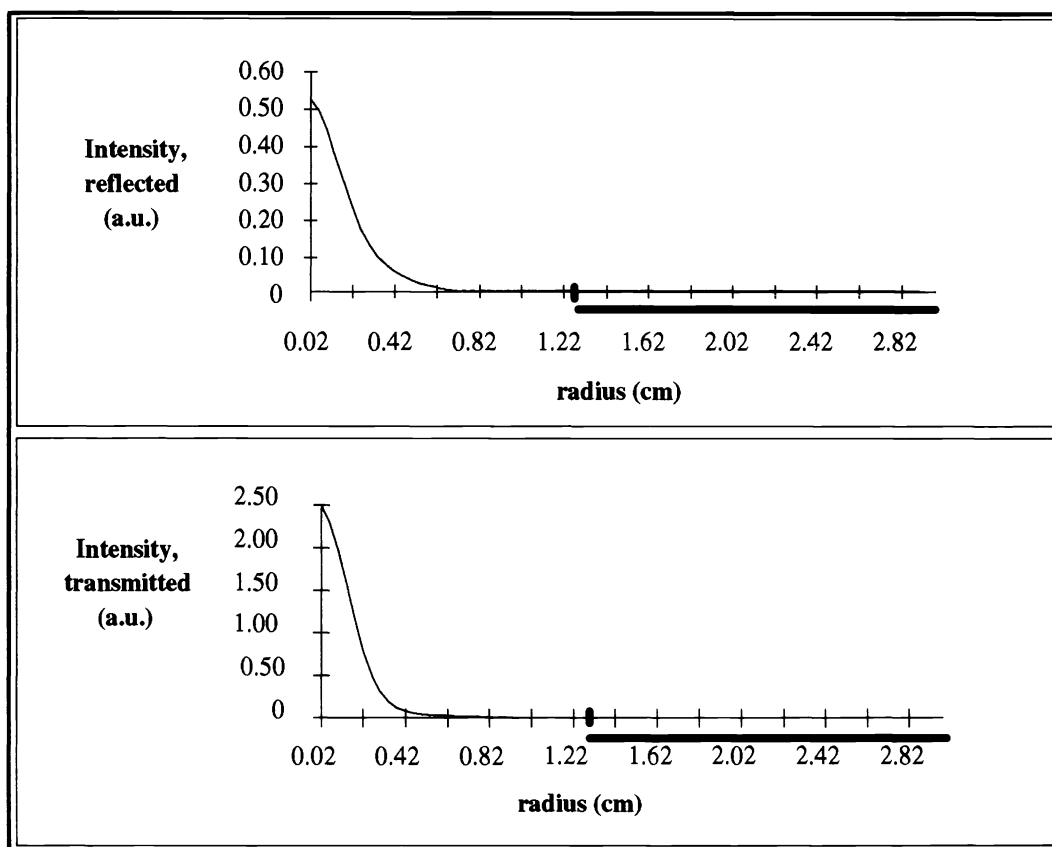


Figure 2. Reflected and transmitted intensity at the surfaces of the tissue slab versus the radius. The thicker lines represent the outer surface of the sphere, which prevents the light from reaching the photo diode.

Figure 3 shows the set-up for the narrow-beam measurements, where the collimated transmittance of the tissue sample was obtained. The light source was the same as for the integrating sphere set-up. By using a more sensitive detector, as a photo multiplier tube, it was possible to spatially filter the light beam from the optical fibre hard and to keep the diameter of the aperture stop in front of the detector as small as 2 millimetres. These two procedures were performed to prevent the scattered light of the tissue sample to be registered as collimated transmitted light. Another action was to keep the distance between the sample and the detector as long as possible, in this case around 60 cm. The collimated transmittance could then be derived as

$$T_{\text{col}} = T_{\text{ND}} \times I_{\text{col}} / I_0$$

where T_{ND} symbols the transmittance of a neutral density filter used when measuring I_0 . I_0 is the light intensity measured by the photo multiplier tube with a reference glass cuvette filled with water at the sample position. I_{col} is the intensity of the light transmitting the tissue sample without any interaction. The attenuation coefficient was obtained by

$$\mu_t = -\ln(T_{\text{col}}) / d$$

with the thickness, d , of the tissue slab.

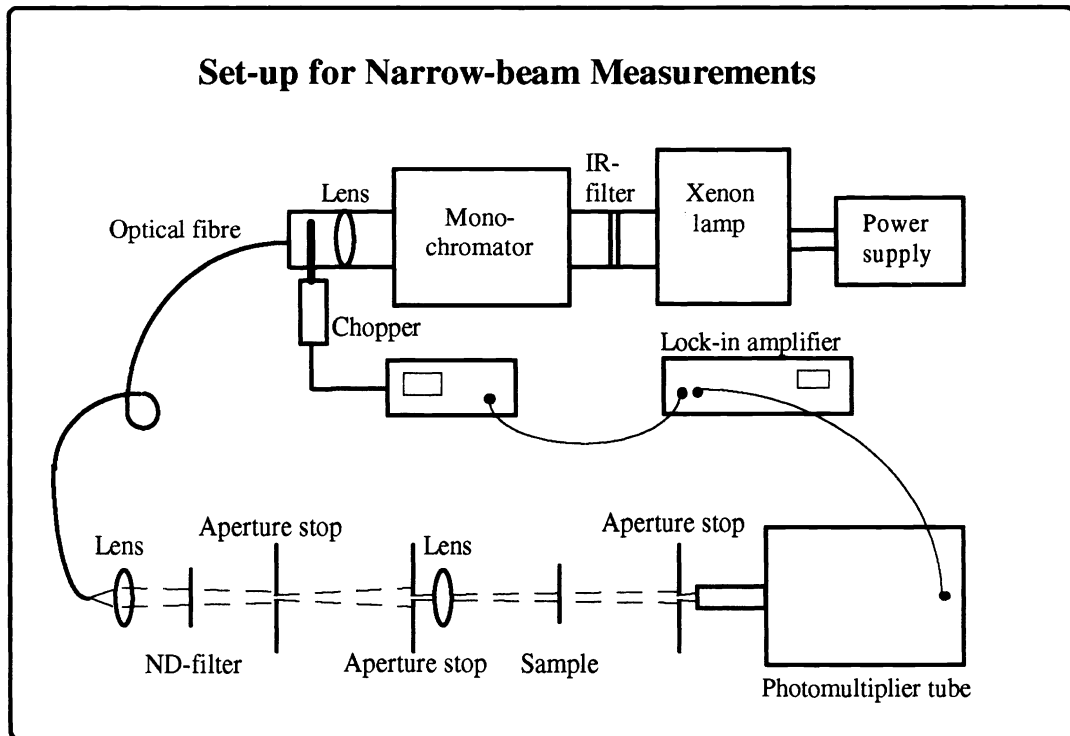


Figure 3. The direct transmittance was measured with a narrow-beam experiment.

2.2 Monte Carlo simulations

Light interaction with tissue can be modelled by Monte Carlo simulations, a random walk for photon packets. The g -factors, scattering and absorption coefficients are defined as well as the thickness of the material layers. A photon packet, given a photon weight, is sent into the tissue and the step size between each interaction position is randomised with a mean step size of $(\mu_s + \mu_a)^{-1}$. At the interaction sites an attenuation of the photon weight is done in proportion to the magnitude of the absorption coefficient, until it falls below a threshold level and the photon packet is terminated. If it is not, the photon packet with its new photon weight is further scattered. The deflection angle, θ , is randomised with the Henyey-Greenstein probability distribution⁵:

$$p(\cos \theta) = (1 - g^2) / (2(1 + g^2 - 2g \cos \theta)^{2/3})$$

This is done until the photon packet reaches either the first or the second boundary and is added to the other reflected or transmitted photons, respectively, yielding the reflectance and transmittance. Monte Carlo simulations link the g -factors, scattering and absorption coefficients to the measured reflectance and transmittance.

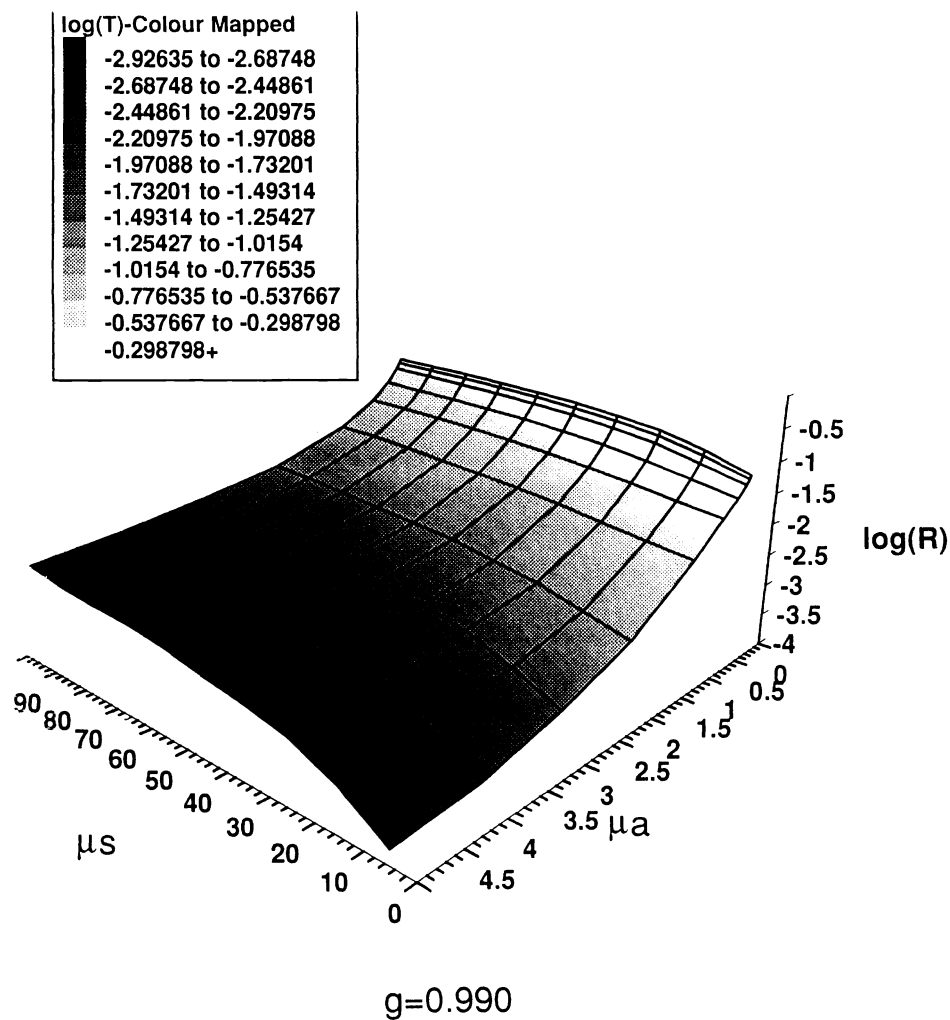


Figure 4. Results of Monte Carlo Simulations presented as log (R) and log (T) versus μ_s and μ_a for $g=0.99$. Log (T) is colour mapped.

We used a Monte Carlo simulation program written by L. Wang and S. L. Jacques⁶ on a DECpc α XP 150-computer. The tissue geometry could be defined as a multilayered medium, in our case a 1 mm thick tissue slab with the refractive index 1.4 in-between two 1 mm thick glass slides with refractive index 1.52. Simulations were performed with 100 000 photon packets for all combinations of 17 g -factors in the range of 0.6 to 0.99, 10 μ_s -coefficients in the range of 5 to 95 mm^{-1} and for 10 μ_a -coefficients in the range of 0.02 to 5 mm^{-1} . The corresponding reflectance and transmittance were arranged in 17 tables, one for each g -factor. An example of these tables, the one for $g=0.990$, is graphically shown in figure 4.

2.3 Interpolation

To find the corresponding g -factor, μ_s and μ_a coefficients to the measured total transmittance and reflectance, a two dimensional spline interpolation of each g -table was

performed. The interpolation resulted in 17 pairs of possible μ_s and μ_a coefficients - one pair for each g-factor table. The result is shown in figure 5.

T-measured: 0.480141		R-measured: 0.154815			
g	μ_s	μ_a	SumSq	T-Interp.	R-Interp.
0.600	-3.657182757	0.111558416	2.38058E-09	0.480141002	0.154814999
0.627	-2.589222086	0.113970411	7.24277E-10	0.480141	0.154815001
0.650	-1.714502963	0.114832985	1.96358E-09	0.480141	0.154815002
0.675	-1.600116122	0.118743187	8.62029E-10	0.480141	0.154815001
0.700	-0.7041435	0.118631863	2.42759E-09	0.480141002	0.154814999
0.725	-0.223778726	0.122013042	2.52929E-09	0.480141002	0.154814999
0.750	0.612495888	0.125180248	2.20827E-09	0.480141002	0.154815001
0.775	1.173940867	0.127384569	4.79625E-09	0.480141004	0.154815002
0.800	2.144582682	0.12912922	4.15582E-10	0.480141	0.154815
0.825	2.911493081	0.135184871	1.35416E-09	0.480140999	0.154815
0.850	4.24378081	0.139258017	9.93728E-10	0.480140999	0.154815
0.875	5.681410449	0.140597094	3.86109E-10	0.480141	0.154815
0.900	7.402347465	0.141528051	9.08169E-11	0.480141	0.154815
0.925	9.578629037	0.142642975	3.37822E-11	0.480141	0.154815
0.950	13.24126037	0.140915085	5.60468E-10	0.480141001	0.154815
0.975	27.01371731	0.137497004	1.85387E-09	0.480141	0.154814998

Figure 5. The result after a two dimensional spline interpolation for T=0.480 and R=0.155 among the Monte Carlo simulated data.

The μ_t coefficient measured at the narrow-beam experiment, was then used to do a one dimensional spline interpolation among these 17 g-factors and their $\mu_s - \mu_a$ pairs. Finally a complete set of optical properties was obtained.

2.4 Calibration

To ensure that the measured optical properties were correct, calibration measurements were performed. The operating procedure was therefore accomplished for a suspension of uniform latex microspheres and ink, yielding measured optical properties between 500 and 800 nm, which were compared with reference values.

0.5 ml latex suspension with 10 % solid plastic spheres and 90 % water was mixed with 2.5 ml ink solution (a mixture of 0.25 ml ink and 100 ml water) and 22 ml water. The latex spheres from Duke Scientific Corporation had the diameter of 0.806 μm . Spherical particles of this size interact with light as Mie scatterers and by Mie calculations the g-factor and the scattering coefficient can be derived⁷. We used a Pascal program by J. R. Zijp and J. J. ten Bosch⁸ to do the Mie computations. The input parameters were the size parameter

$$x=2\pi n_{\text{med}}r/\lambda_{\text{vac}}$$

and the relative refractive index

$$m=n_{\text{part}}/n_{\text{med}}$$

where

- n_{med} - refractive index of the medium surrounding the particles
- n_{part} - refractive index of the particle
- r - radius of the particles
- λ_{vac} - the wavelength of the interacting light in vacuum.

The refractive index, n_{part} , of polystyrene (latex) was found in reference 9

$$n_{\text{part}} = 1.5683 + 10.087 \times 10^{-11} / \lambda_{\text{vac}}^2 \quad (\lambda_{\text{vac}} \text{ in cm})$$

and the density $\rho = 1.057 \pm 0.002 \text{ g/cm}^3$ in reference 10.

The Mie calculations resulted in the g -factor and scattering coefficient of a suspension of latex spheres without any absorber present and the absorption coefficient of the pure ink solution was obtained by absorbance measurements. It was assumed that the ink solution was a pure absorber as well as the latex sphere solution a pure scatterer. Therefore the reference values g , μ_s and μ_a for the mixture of the latex spheres and ink solution was accepted to be the Mie calculated scattering coefficient and g -factor of the latex spheres and the absorption coefficient of the pure ink solution.

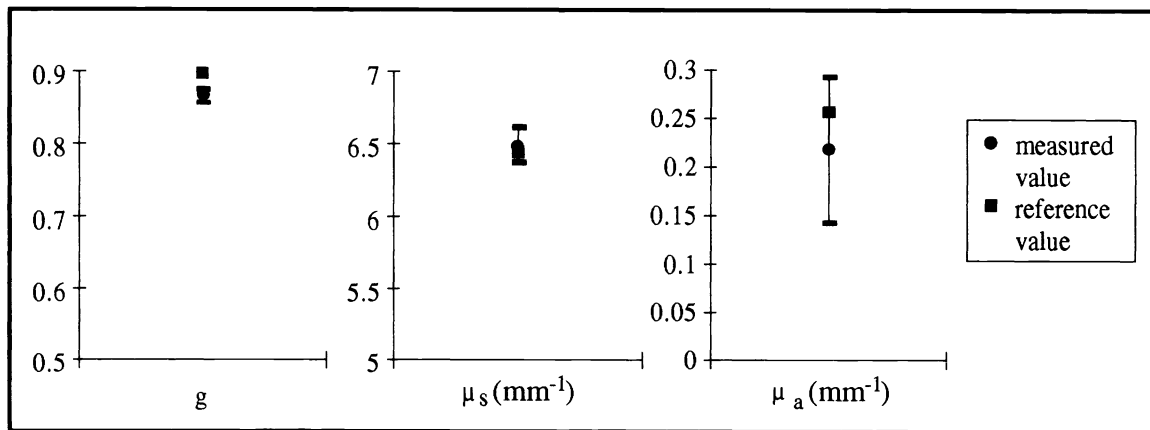


Figure 6. Measured optical properties of the latex sphere - ink solution compared with reference values.

The measured optical properties of the latex sphere and ink solution were compared with the reference values from the Mie calculations and absorbance measurements. The result showed good agreement, see figure 6, particularly for the g -factor and the scattering coefficient, where it was within 1-3%. The absorption coefficients had rather high standard deviation, which other authors¹¹ have commented as a result of the difference in magnitude of the absorption and scattering coefficient. The μ_a -coefficients derived from absorbance measurements of the ink only, were within the limits of the standard deviations.

3. MEASUREMENTS OF TISSUE OPTICAL PROPERTIES IN CONJUNCTION WITH PHOTODYNAMIC THERAPY

Measurements of the optical properties of rat liver tissue, treated with photodynamic therapy, have been performed using the integrating sphere technique described above. The optical properties of the treated and the untreated area were measured and compared.

3.1 Operating procedure

For the experiments nine Sprague-Dawley rats were injected *i.v.* with 30 mg/kg body weight δ -amino-levulinic acid (ALA) 2.5 h prior to the treatment. The abdominal wall of the rat was cut open to expose the liver lobe. A circular region with a diameter of 1.5 cm was irradiated with a light energy density of 60 J/cm² at 635 nm. During the irradiation the power density was kept well below 100 mW/cm² to avoid any hyperthermic effect on the tissue. As a light source a dye laser pumped with an intracavity frequency-doubled Nd:YAG laser, Q-switched at a pulse repetition rate of 4 kHz, was used. Immediately following each irradiation the treated tissue was resected and a 1 mm thick slice of the superficial tissue was cut and placed between two microscope object glasses with 1.0 mm spacers in-between. Two to four minutes after PDT, the optical properties of the treated area followed by an untreated area were derived with the technique described above.

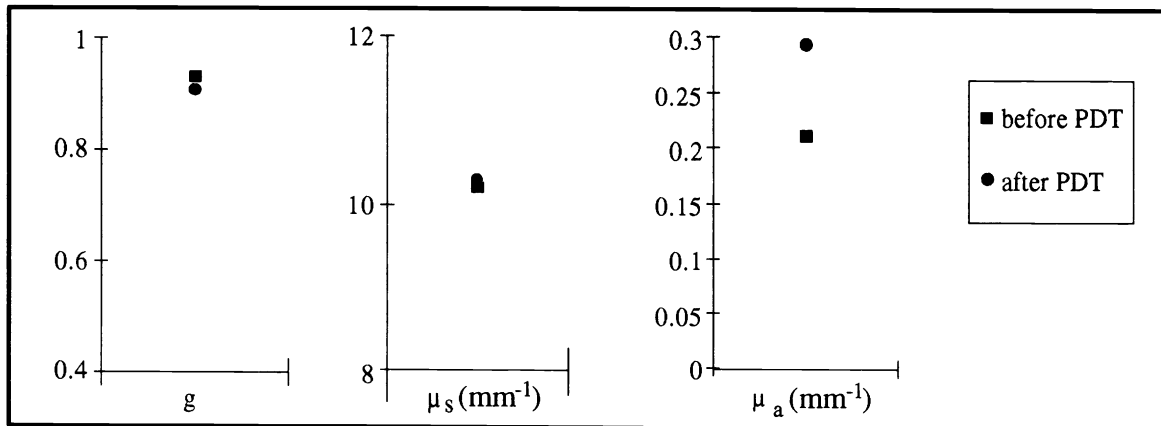


Figure 7. Measured g-factor, scattering and absorption coefficient for a rat liver lobe at 650 nm before and after photodynamic therapy.

3.2 Results

Figure 7 shows typical values of the optical properties at 650 nm, measured before and after PDT, for one of the nine liver lobes. The change of the g-factor in percent, Δg , is calculated as:

$$\Delta g = 100 \times (g_{\text{treated}} - g_{\text{non-treated}}) / g_{\text{non-treated}}$$

and corresponding for $\Delta\mu_s$ and $\Delta\mu_a$. The mean values and standard deviations of the changes for the nine liver samples are shown in figure 8, indicating no change of the g-factor and scattering coefficient. However, the absorption coefficient changed approximately 40 % during the treatment. The standard deviation of the $\Delta\mu_a$ is rather large, which partly can be explained by the small magnitudes of the absorption coefficients.

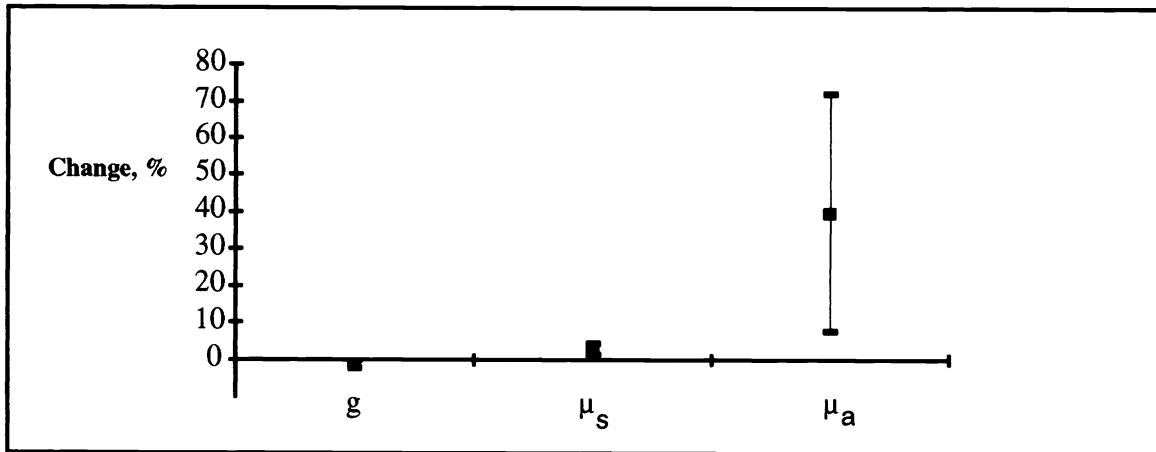


Figure 8. The change of the optical properties at 650 nm during PDT.

4. DISCUSSION

An increasing μ_a coefficient during PDT yields a decreased light penetration, which will affect the treatment. This increase is important to know in order to be able to calculate the light dose in conjunction with the treatment. Further studies are needed to investigate what causes the increased absorption coefficient. One suggestion is that it is due to blood stasis in the treatment region as a result of the treatment.

A. Castellani *et al.* describe in their article¹² the damage of the tissue micro circulation during PDT, which starts with microagglutination of the blood cells followed by blood stasis. The blood vessels turn dilated and full of red blood cells, which most likely leads to higher light absorption. This is in accordance with the increasing absorption coefficient, seen in our experiment.

5. ACKNOWLEDGEMENTS

The authors wish to thank Lexin Liu for obtaining the tissue samples and Anders Persson for helping out with the spline interpolation routine. This work was financially supported by the Swedish research council for engineering sciences. The support from professor Sune Svanberg is gratefully acknowledged.

6. REFERENCES

1. W. -F. Cheong, S. A. Prahl and A. J. Welch, "A review of the optical properties of biological tissues," *IEEE J. Quantum Electron.*, vol. 26, pp. 2166-2185, Dec. 1990.
2. J. W. Pickering, C. J. M. Moes, H. J. C. M. Sterenborg, S. A. Prahl and M. J. C. van Gemert, "Two integrating spheres with an intervening scattering sample," *J. Opt. Soc. Am. A*, vol. 9, pp.621-631, Apr. 1992.
3. V. G. Peters, D. R. Wyman, M. S. Patterson and G. L. Frank, "Optical properties of normal and diseased human breast tissues in the visible and near infrared," *Phys. Med. Biol.*, vol. 35, pp. 1317-1334, 1990.
4. J. H. Torres, A. J. Welch, I. Çilesiz and M. Motamedi, "Tissue optical property measurements: overestimation of absorption coefficient with spectrophotometric techniques," *Lasers Surg. Med.*, vol. 14, pp. 249-257, 1994.
5. L. G. Henyey, J. L. Greenstein, "Diffuse radiation in the galaxy," *Astrophys. J.*, vol. 93, pp. 70-83, 1941.
6. L. Wang and S. L. Jacques, "Monte Carlo modelling of light transport in multi-layered tissues in standard C," University of Texas, M. D. Anderson Cancer Center, 1992.
7. R. Graaff, J. G. Aarnoudse, J. R. Zijp, P. M. A. Slood, F. F.M. de Mul, J. Greve and M. H. Koelink, "Reduced light-scattering properties for mixtures of spherical particles: a simple approximation derived from Mie Calculations," *Appl. Opt.*, vol. 31, pp. 1370-1376, Apr. 1992.
8. J. R. Zijp and J. J. ten Bosch, "Pascal program to perform Mie calculations," *Opt. Engineering*, vol. 32, pp. 1691-1695, July 1993.
9. J. B. Bateman, E. J. Weneck and D. C. Eshler, *J. Coll. Sci.*, vol. 14, pp. 308, 1959.
10. T. L. Pugh and W. Heller, *J. Coll. Sci.*, vol. 12, pp. 173, 1957.
11. R. van Hillegersberg, J. W. Pickering, M. Aalders and J. F. Beek, "Optical Properties of rat liver and tumor at 633 nm and 1064 nm: Photofrin enhances scattering," *Lasers Surg. Med.*, vol. 13, pp. 31-39, 1993.
12. A. Castellani, G. P. Pace and M. Concioli, "Photodynamic effect of haematoporphyrin on blood microcirculation," *J. Path. Bact.*, vol. 86, pp. 99-102, 1963.